REVISION

10th November 2016

Dual-Plate Gold-Gold Microtrench Electrodes for Generator-Collector Voltammetry without Supporting Electrolyte

---

Miguel A. Montiel [1], Jesus Iniesta [1*], Andrew J. Gross [2], Frank Marken [2*]

[1] *Departamento de Química física e Instituto Universitario de Electroquímica, Universidad de Alicante, Apartado 99, 03080 Alicante, Spain*
[2] *Department of Chemistry, University of Bath, Bath, BA2 7AY, UK*

To be submitted to Electrochimica Acta

Proofs to F. Marken

F.Marken@bath.ac.uk

Abstract

A gold-gold dual-plate microtrench electrode system based on two oppositely placed gold surfaces with 5 mm length, 17 μm average depth, and 6 μm inter-electrode gap is employed in generator-collector configuration in a four-electrode cell (counter electrode, reference electrode, and two independent working electrodes denoted "generator" – with scanning potential - and "collector" – with fixed potential). The dual-plate microtrench electrodes were investigated for (i) the reduction of $Ru(NH_3)_6^{3+}$, (ii) the oxidation of ferrocenemethanol, and (iii) the oxidation of iodide in aqueous media, all as a function of supporting electrolyte concentration. It is shown that due to the inter-electrode feedback character of the generator-collector currents, well-defined steady state sensor responses are obtained for the collector electrode even in the absence of added electrolyte. The variation in the mass transport limited steady state current (measured at the collector electrode) with addition/removal of supporting electrolyte remains low (compared to unexpectedly stronger effects caused by the switch between reduction and oxidation conditions at the collector electrode). Microtrench electrode systems are suggested for sensing applications without/with varying levels of supporting electrolyte.

Keywords: ionic strength, diffusion, feedback, sensing, voltammetry.

Graphical Abstract:

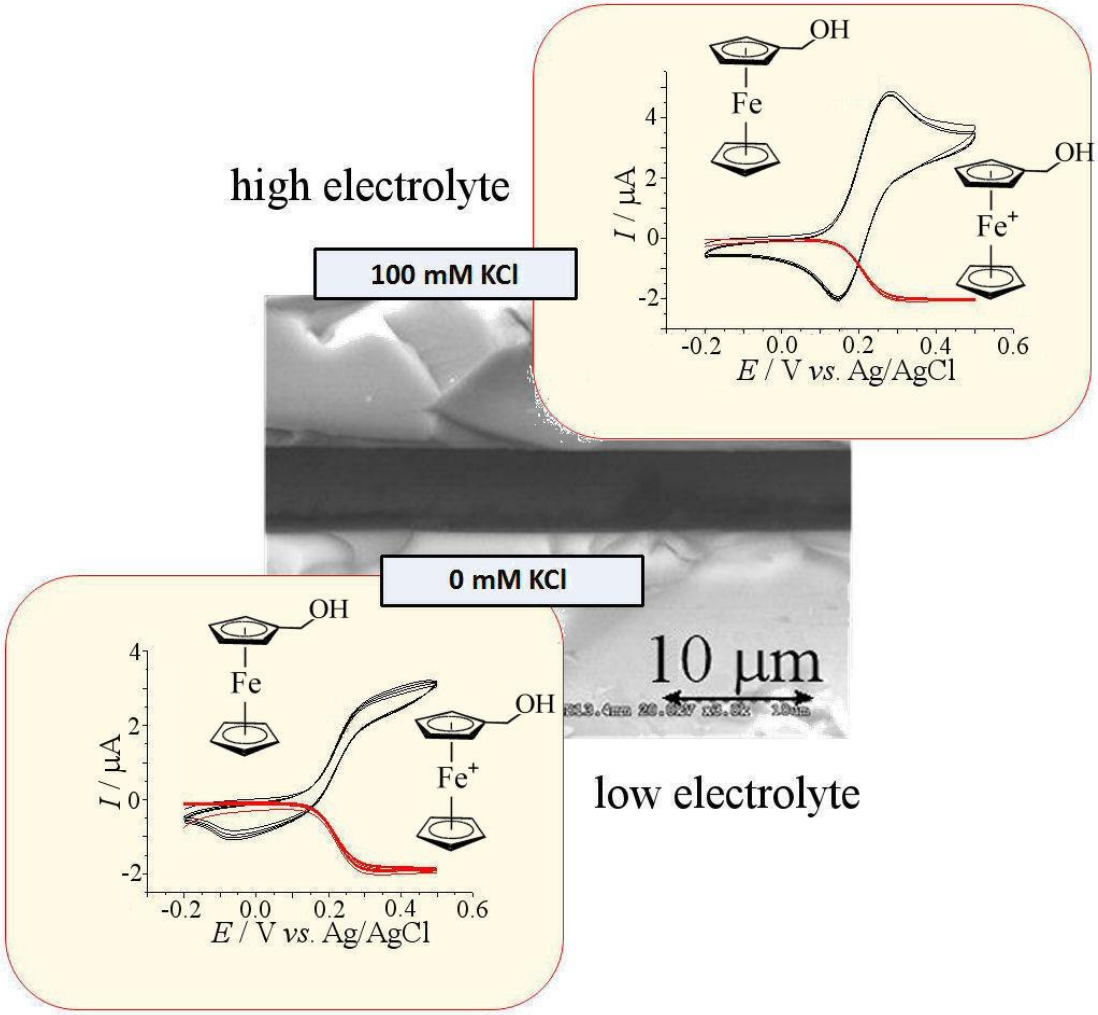

1. Introduction

Dual-plate microtrench electrode systems were introduced in 2013 [1] in an attempt to develop versatile sensor electrodes that allow amplification of redox current responses due to fast feedback *via* inter-electrode diffusion in a small gap similar to microgap electrode systems [2,3,4,5], but with the added advantage of a significantly smaller inter-electrode gap and immediate diffusional access of the sample solution into the open microtrench [6]. Subsequently, this type of electrode has been applied electroanalytically with a silver catalyst for nitrite/nitrate determination [7], with boron-doped diamond electrodes for chloride [8] and sulphide detection [9], as gold-gold microtrench electrode system for cysteine-cystine detection [10], and for the proton/hydrogen redox couple with a platinum-platinum microtrench electrode system [11]. Some benefits of the microtrench electrode configuration are in (i) the application of two (rather than one) electrode potentials simultaneously to provide additional chemical selectivity and signal amplification, (ii) the rejection of irreversible electrode processes such as interfering oxygen reduction or ascorbate oxidation [6], and (iii) the control over the microtrench environment, for example, by *in situ* removal of oxygen and creation of anoxic sensing conditions for sulphide [9]. Most studies performed with dual-plate microtrench electrode systems to date have been carried out in generator-collector feedback mode (with the generator electrode potential sweeping and the collector electrode potential fixed) and in aqueous media, although pulse methods [12] and applications in ionic liquids [13] have also been proposed. In this report, generator-collector voltammetry at a gold-gold dual-plate microtrench electrode system is investigated in the absence of supporting electrolyte.

Generator-collector electrochemistry [14] is commonly applied and useful for a wide range of electroanalytical applications. Rotating ring-disk voltammetry has been frequently employed in catalyst development [15], and microfluidic generator-collector devices have been employed in analysis with hydrodynamic flow [16]. Generator-collector nanogap devices, fabricated using multistep nanofabrication processes, have been developed based entirely on diffusional transport [17] or also coupled with electrokinetic/hydrodynamic flow [18]. Nanogap devices have been improved to the level that they now reach the limit of single molecule electrochemical detection [19]. They also allow the monitoring of bio-catalytic reactions at the single molecule/enzyme level [20]. Bohn and co-workers developed a generator-collector nanogap electrochemical device based on cylindrical pores with two closely-spaced embedded electrodes [21]. These types of nanopore array electrodes, when operated without supporting electrolyte, have recently been shown to result in current enhancements of up to three orders of magnitude possibly due to adsorption/accumulation of redox active species into the pores of the device [22].

In contrast to many single working electrode electroanalytical techniques that have been well-studied and for which there are powerful numerical data analysis software packages, for dual-plate dual-working electrode electroanalytical techniques (in a four-electrode cell) in microtrench devices, there is still a need for better understanding and for theory to be developed. It has been suggested that dual-plate microgap generator-collector electrode experiments can be performed in the absence of intentionally added supporting electrolyte [23] and further theoretical analysis of the simplified case of a closed microgap electrode experiment (configured as a two-electrode cell [24]) led to

the conclusion that complex behaviour can emerge, with mathematical complexity currently preventing access to practical analytical expressions.

In this study, voltammetric experiments are performed with a relatively shallow gold-gold dual-plate microtrench electrode system (the aspect ratio of trench depth: trench width is only 3:1 to avoid additional resistivity from having a deeper trench) immersed in aqueous electrolyte media in the presence of redox-active species. It is shown that for this type of electrode system significant effects from diffusional exchange between the microtrench interior and bulk exterior solution occur. These effects go beyond those observed when adding or removing supporting electrolyte. The $Ru(NH_3)_6^{3+/2+}$, ferrocenemethanol$^{+/0}$, and iodide/tri-iodide/iodine redox systems are investigated and in all cases the effect of supporting electrolyte is evaluated. The effect of supporting electrolyte on the mass transport controlled limiting current appears minor and, as a result, it is proposed that the dual-plate microtrench sensor configuration is relatively insensitive to changes in supporting electrolyte concentration.

2. Experimental

2.1. Reagents. Hydrogen peroxide (30 wt.% in water), ferrocenemethanol (98 %), NaI (>99 %), Na_2SO_4 (anhydrous >99%), and sulfuric acid (≥95–98 %), hydrochloric acid (HCl, 37 %), nitric acid (HNO_3, 70%) from Sigma Aldrich, KCl >99 % from Acros Organics, hexaammineruthenium(III)chloride ($Ru(NH_3)_6Cl_3$, 99%) from Strem Chemicals, and SU-8 2002 series negative photoresist from Microchem Corporation were used as received. Aqueous solutions were prepared using ultrapure water

(demineralised and filtered water taken from a Millipore water purification system) with 18.2 MΩcm resistivity.

2.2. Instrumentation. Electrochemical measurements were performed using a bipotentiostat (CH Instruments CHI910B). A four-electrode cell was employed with a Pt wire counter electrode, Hg/Hg_2SO_4 (sat. K_2SO_4) or Ag/AgCl (1 M KCl) reference electrode, and the two independent working electrodes of the gold-gold microtrench. Measurements were performed at 20 ± 2 °C. A WS-650 Mz-23NPP (Laurell Technologies) spin coater was used to spin photoresist. Scanning electron microscopy (SEM) images were taken with a Hitachi S3000N microscope.

2.3. Electrode Fabrication. The gold-gold dual-plate microtrench electrode was prepared based on the photoresist method developed in previous work for tin-doped indium oxide electrodes [25]. A gold coated (100 nm thickness) glass slide with a titanium adhesion layer (Sigma Aldrich) was cut into two 10 mm × 25 mm pieces. A central 5 mm × 25 mm strip was masked on each substrate using Kapton tape (Farnell, UK) before etching the exposed metal using a solution of aqua regia (1:3 v/v HNO_3: HCl; WARNING: this solution is highly aggressive) for 3 min. After rinsing of the samples in ultrapure water, removing the mask, then drying with a stream of nitrogen, the gold slides were heated at 500 °C for 30 min in air and then cooled to room temperature (the heating destroys the remaining titanium metal film). The gold slides were subsequently spin-coated with a single coat of SU-8 2002 epoxy using a first spin step at 500 rpm (5 s) and a second spin step at 3000 rpm (15 s). The two gold-coated substrates were pressed together face-to-face (see Figure 1). The substrates were placed on a hot-plate pre-heated to 90 °C for 2 min then heated to 160 °C for 5 min. This

effectively glued the two gold surfaces together. After cooling to room temperature the end of the gold-gold electrode system was cut with a diamond blade to reveal the gold-epoxy-gold sandwich. In order to create the microtrench, the epoxy layer is etched away (see Figure 1A) using a piranha etch solution (5:1 sulphuric acid : hydrogen peroxide; *caution, this is a highly aggressive reagent*), and the contacts prepared as previously reported [25]. The duration of the etching process defines the depth of the microtrench.

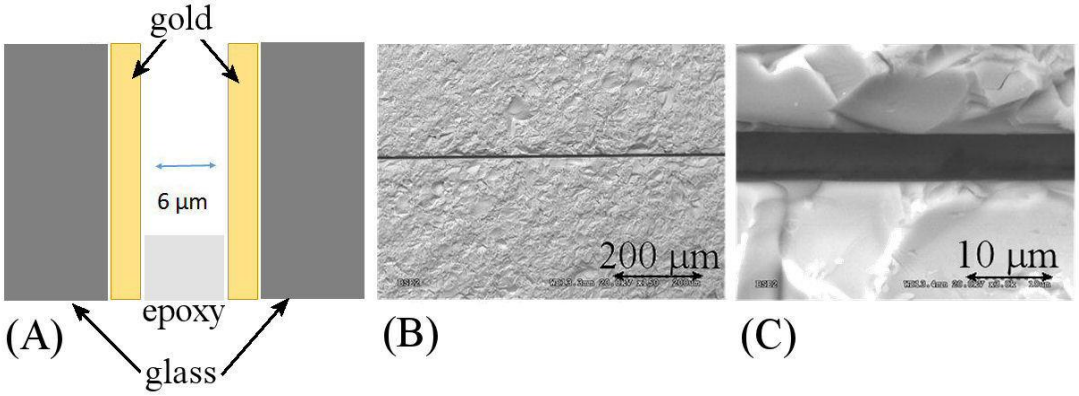

Figure 1. (A) Schematic drawing of the dual-plate gold-gold microtrench electrode system based on two 100 nm gold coated glass slides facing each other. (B,C) Scanning electron microscopy images of the 6 µm wide microtrench.

The 4-electrode electrochemical cell was based on a Pt wire counter electrode, either a Hg/Hg_2SO_4 (with a potential of 0.654 V vs. NHE) or a Ag/AgCl 1 M KCl (with a potential of 0.235 V vs. NHE) reference electrode and a dual-plate gold-gold working electrode combination. If not stated otherwise in cyclic voltammetry experiments, a scan rate of 25 mV s^{-1} was employed and aqueous Na_2SO_4 or KCl was used as supporting electrolyte at varied concentrations (from 0.0 M up to 0.1 M for each supporting electrolyte). The cell volume was 7-8 cm^3 and solutions were thoroughly deoxygenated with a flow of argon (due to hydrophilic gold surfaces there is no problem

with gas bubbles entering the microtrench). The dual-plate gold-gold working electrode system was pre-treated by performing 25 potential cycles in aqueous 0.5 M H_2SO_4 in a potential range from -0.15 to 1.55 V vs. AgCl/Ag (1 M KCl) to clean and recondition the surface.

2.4. Electrode Geometry Calibration. Due to the difficulty of directly measuring the depth of the microtrench, a voltammetric experiment was performed to obtain an estimate. Analysis of the limiting current for the reduction of 1 mM $Ru(NH_3)_6^{3+}$ in aqueous 0.1 M Na_2SO_4 was employed to calibrate the dual-plate microtrench geometry based on a known diffusion coefficient of 0.91×10^{-9} m^2 s^{-1} [26]. From SEM images the inter-electrode gap is estimated as L = 6 μm and the trench length is known to be 5 mm. With equation (1) and a measured limiting current of $I_{lim,supported}$ = 1.26 μA (collector limiting current, *vide infra*) this suggests an average microtrench depth of approximately 17 μm (consistent with an aspect ratio of microtrench depth to inter-electrode gap of approximately 3:1).

$$I_{lim,supported} = \frac{nFADc^0}{L} \qquad (1)$$

Equation 1 describes the steady state diffusional flux between two equidistant planes with gap L, area A (= width × depth), Faraday constant F, number of electrons transferred per molecule diffusing to the electrode surface n, diffusion coefficient D, and concentration difference c^0 based on a simple Nernst diffusion layer [27]. This expression can be used to provide a reference point and as an approximate description of the limiting current for a dual-plate microtrench electrode system (the equation is

strictly valid only for a high aspect ratio of trench depth to inter-electrode gap *L*). The value of the aspect ratio here is relatively low or shallow and as a result the generator current responses in this study often show significant transient current features in addition to the desired steady state current. Nevertheless, the collector current responses show steady-state characteristics and are well-defined and useful for electroanalytical purposes.

3. Results and Discussion

3.1. Supporting Electrolyte Effects on Dual-Plate Sensor Signal I.: Reduction of $Ru(NH_3)_6^{3+}$

The $Ru(NH_3)_6^{3+/2+}$ redox system offers a well-defined one-electron redox system to calibrate the microtrench electrode geometry (*vide supra*) and to explore supporting electrolyte effects (equation 2).

$$Ru(NH_3)_6^{3+} + e^- \rightleftharpoons Ru(NH_3)_6^{2+} \qquad (2)$$

Voltammetric data are summarised in Figure 2. All $E_{1/2}$ values (here defined as $E_{1/2}$ = ½ $E_{p,ox}$ + ½ $E_{p,red}$) values are observed at -0.64 V vs. Hg/Hg_2SO_4 with or without added Na_2SO_4 electrolyte at different concentrations. The left hand column shows the cyclic voltammmogram recorded at only one working electrode with the second working electrode disconnected. Peak features are observed, which are likely to be dominated by diffusion of redox active species from the bulk solution into the microtrench. When comparing data in Figure 2A (no added Na_2SO_4) and Figure 2D (with 0.1 M Na_2SO_4), resistivity effects (Ohmic distortion) at lower supporting electrolyte level are observed. Data in Figure 2B and 2C are consistent with those in Figure 2A and Figure 2D.

When working with both working electrodes (the generator electrode potential scanning and the collector electrode potential fixed) in generator-collector mode, there are two simultaneous current responses shown in black for the generator electrode and shown in red for the collector electrode. Both currents are presented here superimposed into a single plot, but note that the potential scale shows the generator potential with the collector potential being fixed. Generally, for the microtrench electrode system there are two current components due to (i) flow of charge from the microtrench interior to the outside bulk solution (whereby the current flow is "in line" with the external reference electrode and therefore potentially affected by high solution resistivity) and (ii) flow of charge only between the generator and collector (whereby the current flow is "perpendicular" to the reference electrode position and therefore less affected by resistivity). A capacitive current component is observed only for the generator electrode subjected to potential cycling and not for the collector electrode at fixed potential. The steady state current responses recorded here at the collector electrode should be relatively insensitive to solution resistance and free of capacitive effects.

Data shown in the second and third column of Figure 2 correspond to the cases of the collector electrode either being fixed at a potential sufficiently positive to oxidise (at -0.35 V vs. Hg/Hg_2SO_4, forming $Ru(NH_3)_6^{3+}$) or fixed at sufficiently negative potential to reduce (at -0.75 V vs. Hg/Hg_2SO_4, forming $Ru(NH_3)_6^{2+}$), respectively.

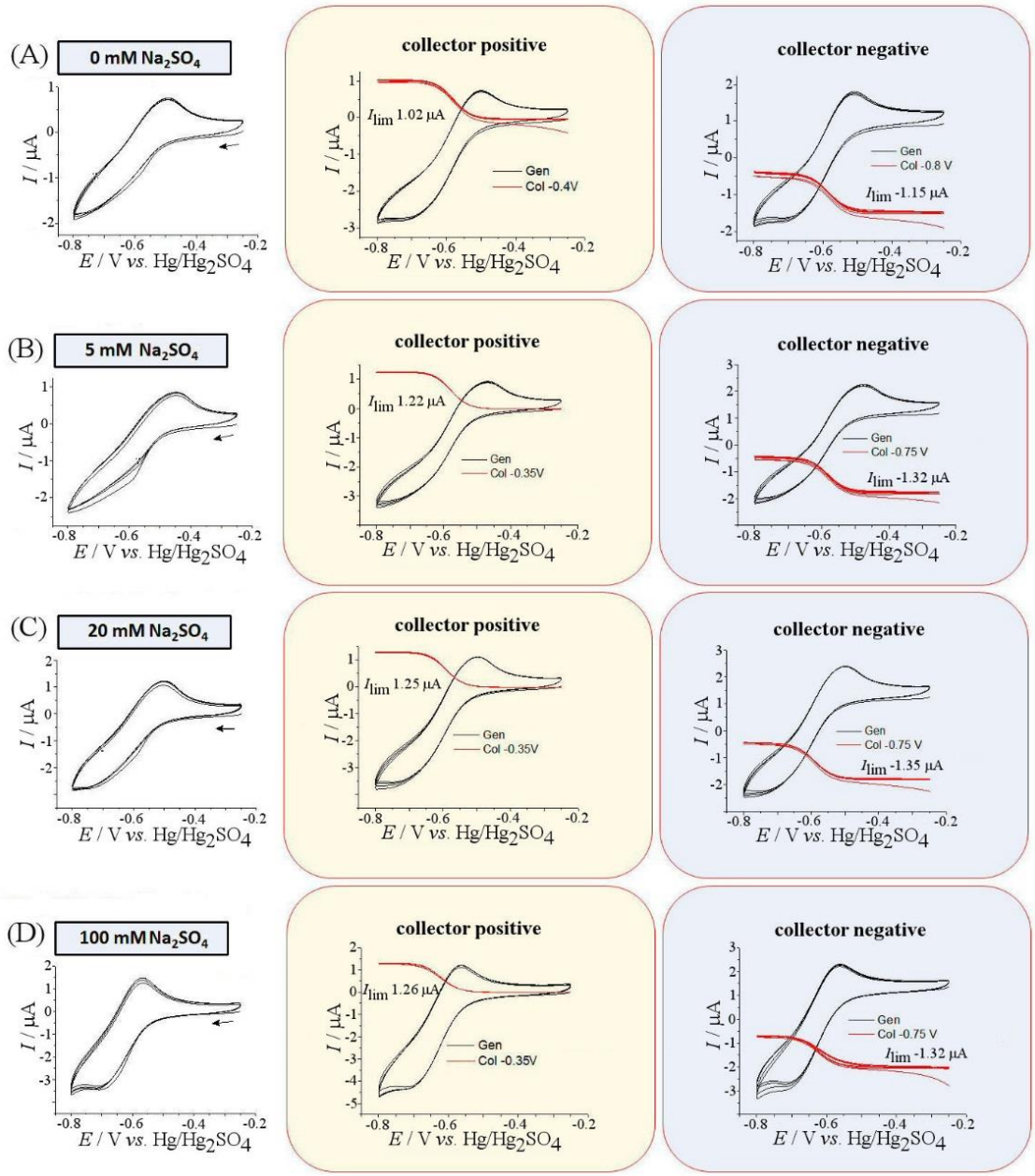

Figure 2. Cyclic voltammograms (scan rate 25 mV s^{-1}; four consecutive potential cycles) for a gold-gold dual-plate microtrench electrode immersed in 1 mM $Ru(NH_3)_6Cl_3$ in aqueous (A) 0, (B) 5, (C) 20, and (D) 100 mM Na_2SO_4. The generator electrode potential is scanning and the collector electrode potential is either floating (left column), set to the positive limit (-0.35 V vs. Hg/Hg_2SO_4, middle column), or set to the negative limit (-0.75 V vs. Hg/Hg_2SO_4, right column).

When holding the collector potential positive (see middle column), the steady state limiting current response is typically 1.26 µA, with high supporting electrolyte

concentration, and reduced to 1.02 μA in the absence of added electrolyte. When holding the collector potential negative (see right column) the resulting limiting current changes from -1.32 μA at high electrolyte level to -1.15 μA at zero added electrolyte concentration. A significant change of ca. 20% in the limiting current appears to occur only at very low supporting electrolyte levels (changing from 5 mM to 0 mM Na_2SO_4). The reason for this change is likely to be connected to migration effects. A further significant effect can be observed when comparing the magnitude of the generator and collector current signals. The generator current always is significantly higher and associated with transient features compared to the collector current, which is smaller and consistent with a steady state response. The main reason for this behaviour is that the fixed potential on the collector electrode causes a "pre-electrolysis" effect associated with a change in the ratio of oxidised to reduced form ($Ru(NH_3)_6^{3+/2+}$) in the bulk solution in the vicinity of the microtrench. Due to the generator electrode potential being continuously scanned, there will always be a "pool" of redox species in the vicinity of the microtrench determined by the fixed collector potential. Therefore, significant differences in steady state voltammetric responses in column 2 and column 3 are seen, and the generator current responses appear higher and more transient compared to the collector current responses, which appear to remain closer to steady state. This also makes the collection efficiency, which is usually defined as the collector limiting current divided by the generator limiting current, ill-defined under these conditions.

3.2. Supporting Electrolyte Effects on Dual-Plate Sensor Signal II.: Oxidation of Ferrocenemethanol

The oxidation of 1 mM ferrocenemethanol was performed in aqueous solution without and with increasing amounts of KCl added as supporting electrolyte. The reversible potential or $E_{1/2}$ value for the one-electron oxidation of ferrocenemethanol [28] (equation 3) is at 0.20 V vs. Ag/AgCl.

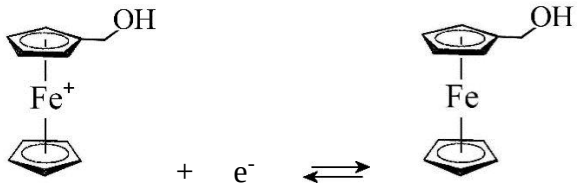

(3)

Cyclic voltammetry data are presented in Figure 3. In the presence of excess supporting electrolyte (Figure 3D) well-defined voltammetric signals are obtained with a collector limiting current of approximately 2.08 μA. With the help of equation 1 the diffusion coefficient can be estimated as 1.4×10^{-9} m^2s^{-1}, which is slightly high compared to literature values 0.8×10^{-9} m^2s^{-1} [29]. The reason for this discrepancy is currently unknown, but may be linked to aggregate formation in the solution phase.

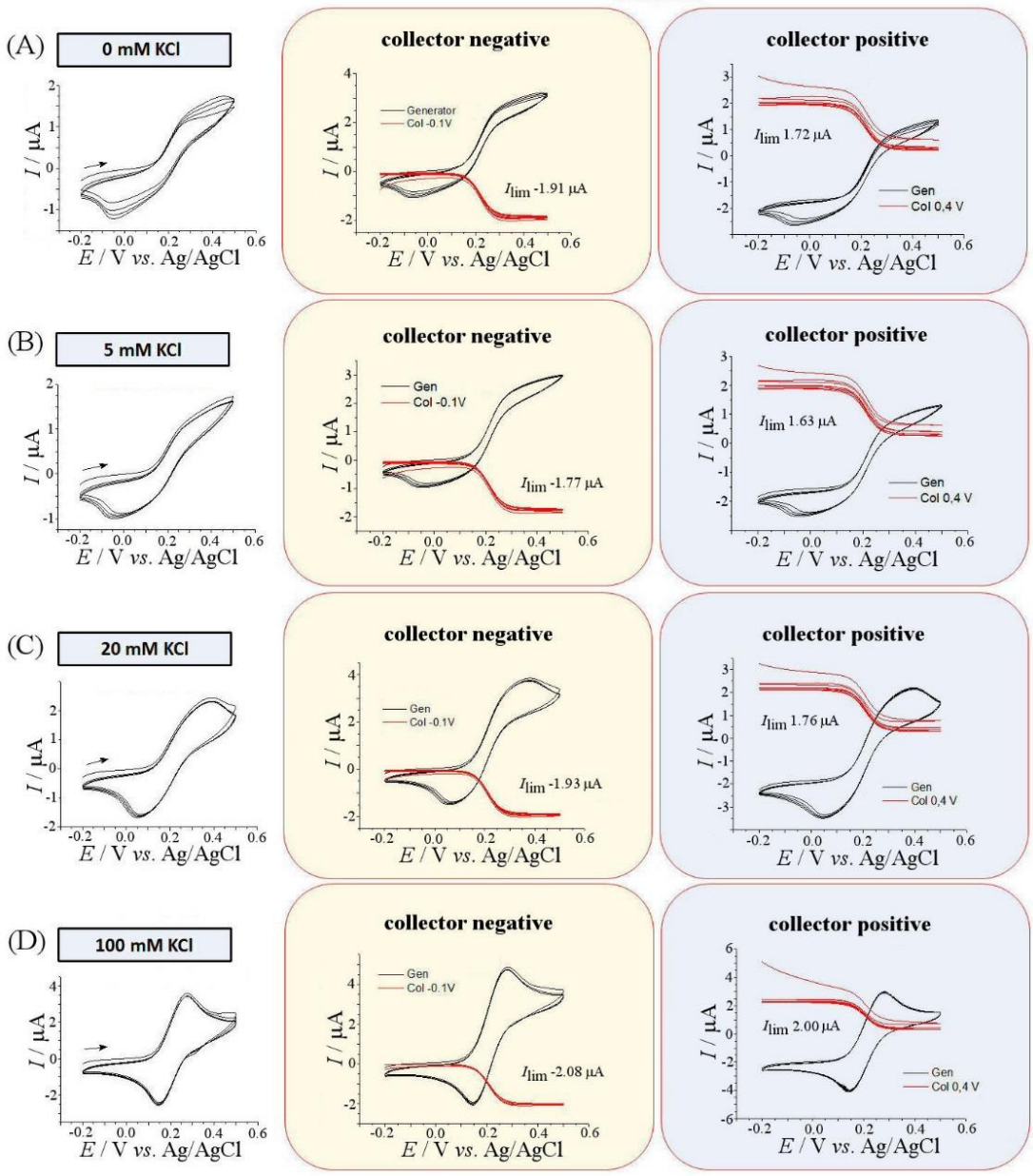

Figure 3. Cyclic voltammograms (scan rate 25 mV s^{-1}, four consecutive potential cycles) for a gold-gold dual-plate microtrench electrode immersed in 1 mM ferrocenemethanol in aqueous (A) 0, (B) 5, (C) 20, and (D) 100 mM KCl. The generator electrode potential is scanning and the collector electrode potential is either floating (left column), set to the negative limit (-0.2 V vs. Ag/AgCl, middle column), or set to the positive limit (+0.5 V vs. Ag/AgCl, right column).

When lowering the concentration of the supporting electrolyte, limiting current values are slightly lowered (just as in the case of the reduction of $Ru(NH_3)_6^{3+}$, see Figure 2). However, limiting current values (as determined at the collector electrode) generally

remain very similar. When the anodic process occurs at the collector electrode (with E_{col} = 0.4 V vs. Ag/AgCl; 3rd column), limiting currents seem slightly lower compared to the case of the cathodic process occurring at the collector (with E_{col} = -0.1 V vs. Ag/AgCl; 2nd column). This trend seems opposite to that seen for reduction of $Ru(NH_3)_6^{3+}$, but for both systems the lower current is associated with the electrode reaction producing the more highly charged species. The lower diffusion coefficient of the more highly charged species in combination with the more complex diffusion geometry in the shallow (only 17 μm deep) microtrench are likely to be responsible for the observed effects.

Next, the oxidation of ferrocenemethanol was investigated in the presence of Na_2SO_4 electrolyte. Figure 4A to 4D show data for increasing amounts of added supporting electrolyte. Perhaps surprisingly, in this case the limiting currents in the presence of excess electrolyte are lower compared to those in the absence of intentionally added electrolyte. This implies an effect of the electrolyte anion (here doubly charged sulphate). Limiting currents in the absence of supporting electrolyte agree between the two sets of experiments (although for the neutral ferrocenemethanol without electrolyte potentially trace salt impurities may have to be considered), but with added electrolyte the opposite trends are seen compared to the $Ru(NH_3)_6^{3+/2+}$ redox system. Initial transient behaviour of the collector electrode during consecutive potential cycles (when positive potentials are applied at the collector) are linked to non-steady state processes and diffusion of species from the bulk solution outside of the microtrench into the inter-electrode gap. Overall, limiting currents remain similar as the level of electrolyte is altered (to within 20 %).

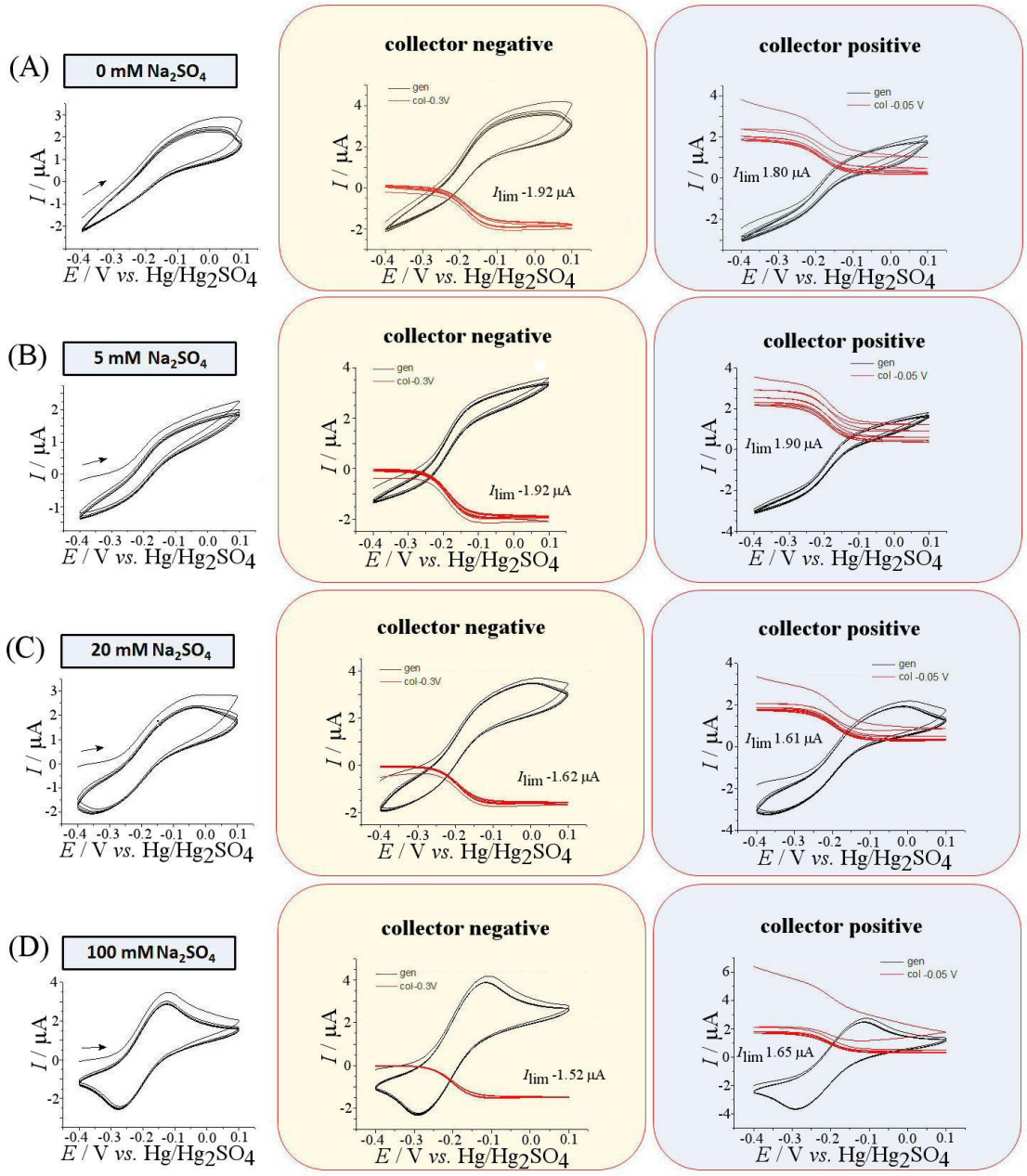

Figure 4. Cyclic voltammograms (scan rate 25 mV s^{-1}, four consecutive potential cycles) for a gold-gold dual-plate microtrench electrode immersed in 1 mM ferrocenemethanol in aqueous (A) 0, (B) 5, (C) 20, and (D) 100 mM Na_2SO_4. The generator electrode potential is scanning and the collector electrode potential is either floating (left column), set to the negative limit (-0.3 V vs. Hg/Hg_2SO_4, middle column), or set to the positive limit (-0.05 V vs. Hg/Hg_2SO_4, right column).

3.3. Supporting Electrolyte Effects on Dual-Plate Sensor Signal III.: Oxidation of Iodide to Iodine

The iodide/iodine redox system in aqueous Na_2SO_4 offers a more complex chemical system with formation of a neutral product (in contrast to the ferrocenemethanol where the neutral molecule is converted into a cation, for example). The oxidation of iodide is known to proceed in two steps with a tri-iodide, I_3^-, intermediate that can often be detected [30]. Here, the iodide oxidation is dominated by the direct formation of I_2 with only little direct voltammetric evidence for intermediate species (apart from a more complicated wave shape). Therefore, the reaction equation is simplified as shown in equation 4.

$$I_2 + 2\,e^- \rightleftharpoons 2\,I^- \qquad (4)$$

Figure 5 shows voltammetric data for a floating microtrench (only one electrode connected), for a negative collector potential (E_{col} = -0.20 V vs. Hg/Hg_2SO_4; 2nd column), and for a positive collector potential (E_{col} = 0.25 V vs. Hg/Hg_2SO_4; 3rd column). With the collector held at negative potentials, the limiting current is typically 2.7 μA, independent of added supporting electrolyte levels. This corresponds to an estimated diffusion coefficient (based on equation 1) of 1.9×10^{-9} m^2s^{-1}, which is in good agreement compared to the literature value for iodide (2.0×10^{-9} m^2s^{-1} [31]). Also note the change in shape of the generator current responses, which are closer to steady state due to the faster rate of diffusion. However, when investigating the case for the collector potential held positive, the limiting currents are consistently higher at 4.1 μA (independent of supporting electrolyte concentration). This increase is significant and again associated with the positive potential being applied to the collector electrode. The diffusion coefficient for I_2 (1.3×10^{-9} m^2s^{-1} [32]) can be expected to be much lower compared to that for I^-. Therefore, an effect associated with a change in the diffusion

behaviour in combination with the complicated geometry of the shallow microtrench has to be considered.

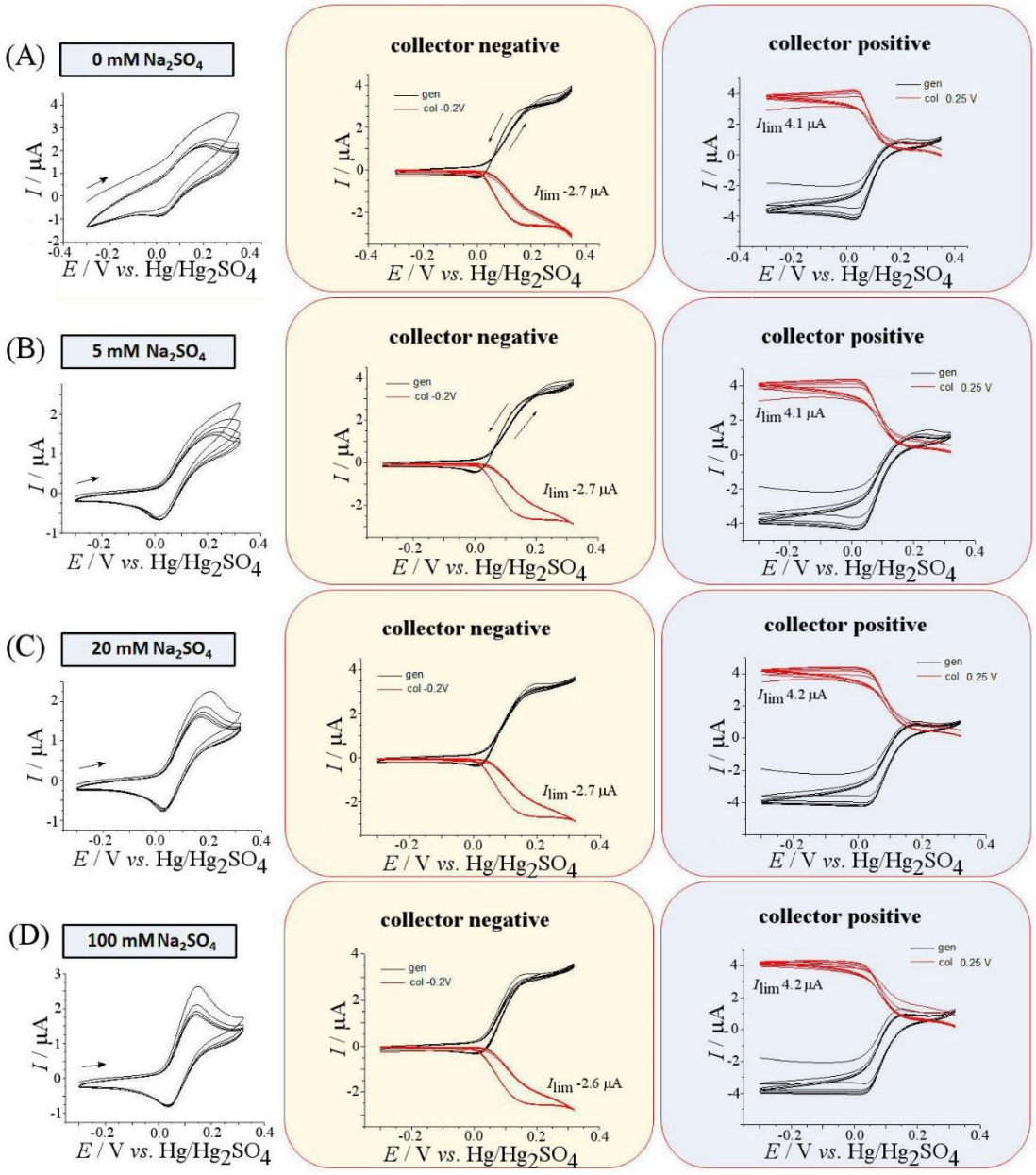

Figure 5. Cyclic voltammograms (scan rate 25 mV s^{-1}, four consecutive potential cycles) for a gold-gold dual-plate microtrench electrode immersed in 1 mM NaI in aqueous (A) 0, (B) 5, (C) 20, and (D) 100 mM Na_2SO_4. The generator electrode potential is scanning and the collector electrode potential is either floating (left column), set to the negative limit (-0.2 V vs. Hg/Hg_2SO_4, middle column), or set to the positive limit (0.25 V vs. Hg/Hg_2SO_4, right column).

When comparing the relative magnitude of generator and collector currents in the data shown in Figure 5, it can be observed that in all cases non-steady state behaviour is seen (mainly at the generator) and the collector current appears always lower compared to the generator current. Similar trends were also observed in the data for the reduction of $Ru(NH_3)_6^{3+}$ and for the oxidation of ferrocenemethanol. The reason for this trend is the pre-electrolysis of bulk solution outside of the microtrench at the fixed collector potential and a process at the generator electrode that is always working against this pre-electrolysis. That is, for the case of iodide/iodine the bulk solution phase outside of the microtrench is dominated by iodide for E_{col} = -0.2 V vs. Hg/Hg_2SO_4 and dominated by iodine and triiodide for E_{col} = 0.25 V vs. Hg/Hg_2SO_4. Diffusional processes associated with the shallow microtrench geometry clearly outweigh any effects due to supporting electrolyte. A more quantitative understanding of the steady state limiting currents will require more experimental work including chronoamperometry to reach longer time domains, and simulation of diffusion-migration processes taking into account both dual-plate microtrench inter-electrode transport and transport from the bulk solution outside of the microtrench.

4. Conclusions

It has been demonstrated that a dual-plate microtrench electrode system based on two gold coated glass slides with 6 μm gap, 17 μm depth, and with 5 mm length offers a robust electroanalysis tool potentially useful, for example, for detection of physiological analytes of interest such as iodide without intentional addition of supporting electrolyte. In particular, the shallow microtrench can be suggested to be associated with significant levels of diffusional exchange between the microtrench

interior and with the exterior bulk solution, and additional complexity in signals when comparing data obtained with fixed collector potentials set at positive and negative potentials for oxidation and for reduction, respectively. Deeper microtrenches will provide a better/more stable apparent steady state (although diffusional exchange with the outside solution will take longer) and could be studied in future to further optimise sensor performance. Depending on the type of analysis task, it may also be beneficial to employ other types of electrode materials. The effect of supporting electrolyte has been investigated and, although some detrimental effects of low support ratios on the generator signal were apparent, well-defined steady state collector current responses were observed in all cases. The effects of varying/removing the supporting electrolyte appeared to remain relatively small.

In future, it will be interesting to apply this type of generator-collector electrode for sensing in physiological samples and also in sensors operating in resistive non-aqueous media. Development of improved experiments (with deeper microtrench devices) and quantitative theory based on advanced numerical simulation methods will be possible. Microtrench electrode systems could provide an interesting alternative to conventional electrode systems also in organic/oil biphasic systems. When lowering the inter-electrode gap towards nanotrench systems, electroanalysis at extremely low concentration levels for example in oils could become feasible.

Acknowledgements

A.J.G and F.M gratefully acknowledge the Engineering and Physical Sciences Research Council (EP/I028706/1) for financial support. M.A.M and J.I. thank the

MICINN-FEDER for financial support (CTQ2013-48280-C3-3-R). We thank Professor Keith B. Oldham for helpful discussion.

References

[1] S.E.C. Dale, Y.H. Chan, P.C.B. Page, E.O. Barnes, R.G. Compton, F. Marken, A gold-gold oil microtrench electrode for liquid-liquid anion transfer voltammetry, Electrophoresis 34 (2013) 1979-1984.

[2] C.R. Christensen, F.C. Anson, Chronopotentiometry in thin layers of solution, Anal. Chem. 35 (1963) 205-206.

[3] L. Rassaei, F. Marken, Pulse-voltammetric glucose detection at gold junction electrodes, Anal. Chem. 82 (2010) 7063-7067.

[4] L.B. Anderson, C.N. Reilley, Thin-layer electrochemistry – use of twin working electrodes for study of chemical kinetics, J. Electroanal. Chem. 10 (1965) 538-539.

[5] A.T. Hubbard, D.G. Peters, Electrochemistry in thin layers of solution, Crit. Rev. Anal. Chem. 3 (1973) 201-242.

[6] M.A. Hasnat, A.J. Gross, S.E.C. Dale, E.O. Barnes, R.G. Compton, F. Marken, A dual-plate ITO-ITO generator-collector microtrench sensor: surface activation, spatial separation and suppression of irreversible oxygen and ascorbate interference, Analyst 139 (2014) 569-575.

[7] A.J. Gross, S. Holmes, S.E.C. Dale, M.J. Smallwood, S.J. Green, C.P. Winlove, N. Benjamin, P.G. Winyard, F. Marken, Nitrite/nitrate detection in serum based on dual-plate generator-collector currents in a microtrench, Talanta 131 (2015) 228-235.

[8] A.J. Gross, F. Marken, Boron-doped diamond dual-plate microtrench electrode for generator-collector chloride/chlorine sensing, Electrochem. Commun. 46 (2014) 120-123.

[9] H.M. Harvey, A.J. Gross, P. Brooksby, A.J. Downard, S.J. Green, C.P. Winlove, N. Benjamin, P.G. Winyard, M. Whiteman, J.L. Hammond, P. Estrela, F.

Marken, Boron-doped diamond dual-plate deep-microtrench device for generator-collector sulfide sensing electroanalysis 27 (2015) 2645-2653.
[10] J.L. Hammond, A.J. Gross, P. Estrela, J. Iniesta, S.J. Green, C.P. Winlove, P.G. Winyard, N. Benjamin, F. Marken, Cysteine-cystine redox cycling in a gold-gold dual-plate generator-collector microtrench sensor, Anal. Chem. 86 (2014) 6748-6752.
[11] S.E.C. Dale, A. Vuorema, M. Sillanpaa, J. Weber, A.J. Wain, E.O. Barnes, R.G. Compton, F. Marken, Nano-litre proton/hydrogen titration in a dual-plate platinum-platinum generator-collector electrode micro-trench, Electrochim. Acta 125 (2014) 94-100.
[12] S.E.C. Dale, F. Marken, Pulse electroanalysis at gold-gold micro-trench electrodes: chemical signal filtering, Faraday Disc. 164 (2013) 349-359.
[13] M.A. Montiel, J. Iniesta, A.J. Gross, T. Thiemann, F. Marken, Generator-collector voltammetry at dual-plate gold-gold microtrench electrodes as diagnostic tool in ionic liquids, Electroanalysis 28 (2016) 1068-1076.
[14] E.O. Barnes, G.E.M. Lewis, S.E.C. Dale, F. Marken, R.G. Compton, Generator-collector double electrode systems: a review, Analyst 137 (2012) 1068-1081.
[15] W.J. Albery, M.L. Hitchman, Ring-disc Electrodes, Clarendon Press, Oxford, 1971.
[16] C. Amatore, N. Da Mota, C. Lemmer, C. Pebay, C. Sella, L. Thouin, Theory and experiments of transport at channel microband electrodes under laminar flows. 2. electrochemical regimes at double microband assemblies under steady state, Anal. Chem. 80 (2008) 9483-9490.
[17] E. Kätelhön, B. Hofmann, S.G. Lemay, M.A.G. Zevenbergen, A. Offenhausser, B. Wolfrum, Nanocavity redox cycling sensors for the detection of dopamine fluctuations in microfluidic gradients, Anal. Chem. 82 (2010) 8502-8509.
[18] K. Mathwig, S.G. Lemay, Mass transport in electrochemical nanogap sensors, Electrochim. Acta 112 (2013) 943-949.
[19] K. Mathwig, T.J. Aartsma, G.W. Canters, S.G. Lemay, Nanoscale methods for single-molecule electrochemistry, Ann. Rev. Anal. Chem. 7 (2014) 383-404.
[20] K. Mathwig, Q.J. Chi, S.G. Lemay, L. Rassaei, Handling and sensing of single enzyme molecules: from fluorescence detection towards nanoscale electrical measurements, ChemPhysChem 17 (2016) 452-457.

[21] C.X. Ma, N.M. Contento, P.W. Bohn, Redox cycling on recessed ring-disk nanoelectrode arrays in the absence of supporting electrolyte, J. Amer. Chem. Soc. 136 (2014) 7225-7228.
[22] C.X. Ma, W. Xu, W.R.A. Wichert, P.W. Bohn, Ion accumulation and migration effects on redox cycling in nanopore electrode arrays at low ionic strength, ACS Nano 10 (2016) 3658-3664.
[23] W. Hyk, Z. Stojek, Thin and ultra-thin layer dual electrode electrochemistry: theory of steady-state voltammetry without supporting electrolyte, Electrochem. Commun. 34 (2013) 192-195.
[24] K.B. Oldham, F. Marken, J.C. Myland, Theory of unsupported, steady-state, Nernstian, three-ion, twin-electrode, voltammetry:the special case of dual concentration polarization, J. Solid State Electrochem. 20 (2016) 3083-3095.
[25] A.J. Gross, F. Marken, ITO-ITO dual-plate microgap electrodes: E and EC' generator-collector processes, Electroanalysis 27 (2015) 1035-1042.
[26] F. Marken, J.C. Eklund, R.G. Compton, Voltammetry in the presence of ultrasound – can ultrasound modify heterogeneous electron-transfer kinetics, J. Electroanal. Chem. 395 (1995) 335-339.
[27] R.G. Compton, C.E. Banks, Understanding voltammetry, Imperial College Press, London 2011, p. 94.
[28] C.Y. Lee, D. Elton, A. Brajter-Toth, A.M. Bond, Attributes of large-amplitude Fourier transformed alternating current voltammetry at array and single carbon fiber microdisk electrodes, Electroanalysis 25 (2013) 931-944.
[29] A.P. O'Mullane, J. Zhang, A. Brajter-Toth, A.M. Bond, Higher harmonic large-amplitude Fourier transformed alternating current voltammetry: analytical attributes derived from studies of the oxidation of ferrocenemethanol and uric acid at a glassy carbon electrode, Anal. Chem. 80 (2008) 4614-4626.
[30] E.I. Rogers, D.S. Silvester, L. Aldous, C. Hardacre, R.G. Compton, Electrooxidation of the iodides [C(4)mim]I, LiI, NaI, KI, RbI, and CsI in the room temperature ionic liquid [C(4)mim][NTf2], J. Phys. Chem. C 112 (2008) 6551-6557.
[31] F. Marken, R.P. Akkermans, R.G. Compton, Voltammetry in the presence of ultrasound: the limit of acoustic streaming induced diffusion layer thinning and the effect of solvent viscosity, J. Electroanal. Chem. 415 (1996) 55-63.
[32] L. Cantrel, R. Chaouche, J. Chopin-Dumas, Diffusion coefficients of molecular iodine in aqueous solutions, J. Chem. Eng. Data 42 (1997) 216-220.